INSTITUTE OF PHYSICS PUBLISHING JOURNAL OF PHYSICS B: ATOMIC, MOLECULAR AND OPTICAL PHYSICS

J. Phys. B: At. Mol. Opt. Phys. **36** (2003) 2099–2109 PII: S0953-4075(03)58272-4

Foreign gas pressure broadening and shifts of the 2S–4S two-photon transition in lithium

W DeGraffenreid[1], **Sarah C Campbell**[2] **and Craig J Sansonetti**

National Institute of Standards and Technology, Gaithersburg, MD 20899-8422, USA

E-mail: degraff@csus.edu and craig.sansonetti@nist.gov

Received 8 January 2003, in final form 4 April 2003
Published 7 May 2003
Online at stacks.iop.org/JPhysB/36/2099

Abstract

We have observed broadening and shift of the 2S–4S Doppler-free two-photon transition of atomic Li by collisions with neon and argon buffer gases in a heat-pipe oven. Measured broadening and shift rates are presented and compared with theoretical predictions calculated in the impact approximation using three different interaction potentials. A superposition of polarization and modified Fermi potentials gives good agreement with the experimental data.

1. Introduction

In recent years, there have been rapid advances in theoretical models and calculational techniques for few-electron atoms. Specifically, lithium and lithium-like ions have become a field of intense activity. Recent review articles by King [1, 2] summarize the development of the theory over the past decade. Rapid advances in the calculation of energy levels, ionization potential, fine and hyperfine structure and isotope shifts have created a need for improved experimental data to test theory.

While lithium is attractive to theorists because of its simplicity, it is the most difficult of the alkali metals for experimentalists. Lithium rapidly attacks and darkens most glasses, rendering simple vapour cells of little use. For this reason, experiments are frequently performed in heat-pipe ovens with non-reactive buffer gases such as neon and argon. To concentrate the Li atoms at the centre of the pipe and away from the viewports, the centre of the pipe is heated and the ends are cooled. Collisions between the hot Li and the cold buffer gas prevent diffusion of the Li to the cell windows.

In recent attempts to measure the transition energy, isotope shift and hyperfine structure of the Li 2S–4S transition in a heat pipe, we observed that the presence of the buffer gas, even at background pressures as low as 50 Pa (0.375 Torr), caused significant foreign gas shifts and line broadening. In this paper, we present precise determinations of the rates for pressure broadening and shift of the 2S–4S transition by neon and argon.

[1] Present address: California State University, Sacramento, Sacramento, CA 95819-6041, USA.
[2] Present address: SUNY Stony Brook, Stony Brook, NY 11794-3800, USA.

 © 2003 IOP Publishing Ltd Printed in the UK

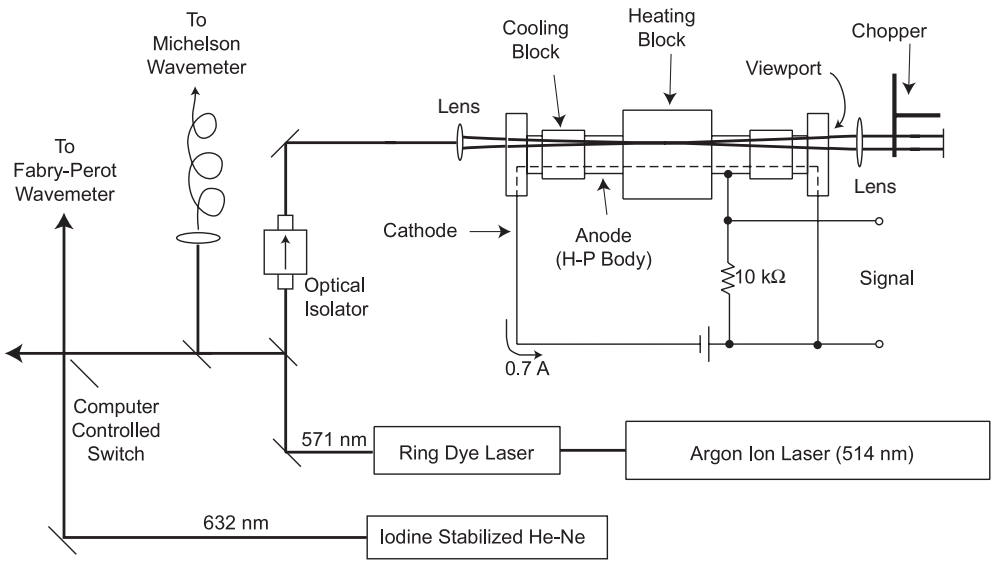

Figure 1. Schematic diagram of the experimental layout. The thermionic signal is AC coupled to a lock-in amplifier.

2. Experiment

Our experimental apparatus for measuring two-photon transitions in Li is shown in figure 1. The Li source is a heat-pipe thermionic diode [3] that is filled with argon or neon buffer gas. The pipe is connected to a large vacuum manifold at room temperature. The centre of the pipe is heated to approximately 680 °C by an oven consisting of nichrome wire threaded through ceramic rods. The wire is wound to minimize stray magnetic fields within the pipe. The ends of the pipe are cooled with coils through which 20 °C water flows. Lithium vaporizes in the hot centre and diffuses toward the cool ends, where collisions with the cold walls and cool buffer gas cause the Li vapour to condense before reaching the glass viewports. A stainless steel wire mesh lines the inside of the pipe, allowing capillary flow of liquid lithium from the ends to the centre. The heat pipe was loaded with approximately 5 g of natural lithium.

Laser-excited atoms in the heat pipe are detected with a thermionic diode [3]. A 0.1 mm diameter tungsten cathode filament is positioned through one side of the heat pipe, and the laser beam is directed through the other. The filament and the laser beam are separated by a vertical tungsten wire grid in the centre of the pipe, that shields the atoms in the laser interaction region from stray fields generated by the filament. A current-regulated power supply provides the 0.7 A filament current. The laser beam is modulated at 190 Hz by an optical chopper, and the synchronous variation of the thermionic diode current is detected with a lock-in amplifier.

A single-frequency ring dye laser with rhodamine 6G dye provides approximately 550 mW of power at 571 nm (half the 2S–4S transition energy). The beam passes through an optical isolator to prevent feedback to the laser cavity and is steered to the heat pipe. A lens with 50 cm focal length focuses the laser beam to a waist near the centre of the tube. The beam is retro-reflected and refocused with a plane mirror and a second 50 cm lens. Considering losses at optical surfaces, we estimate the laser intensity at the beam waist to be approximately 3×10^7 W m^{-2}. The laser is linearly polarized and has a line width of approximately 1 MHz.

A small portion of the laser beam is diverted to two wavemeters. Approximately half of the diverted power is sent via an optical fibre to a fringe counting Michelson wavemeter. This wavemeter is referenced to a commercial frequency-stabilized He–Ne laser and has an overall

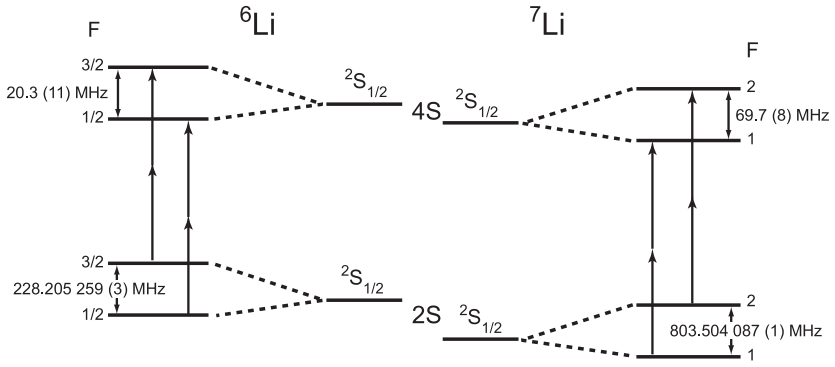

Figure 2. Hyperfine structure for the 2s and 4s states of lithium. The ground state hyperfine splittings are from [9]. The excited state splittings are from [10].

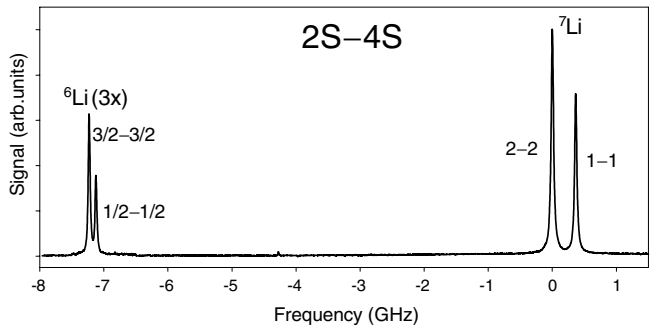

Figure 3. Laser scan containing all four allowed transitions. The frequency scale is the detuning of the laser from the ^{7}Li 2–2 transition. The ^{6}Li lines have been scaled by a factor of three.

uncertainty of about 0.002 cm^{-1}. The Michelson wavemeter is used to tune the dye laser to the desired wavelength region and to make initial measurements of the two-photon transitions. The remaining portion of the diverted beam is directed to a Fabry–Perot wavemeter [4–6], which is referenced to an I_2-stabilized He–Ne laser that is accurate to a few parts in 10^{10} [7, 8]. The overall uncertainty of measurements made with the Fabry–Perot wavemeter is a few parts in 10^9.

The $^2S_{1/2}$ states of ^{6}Li and ^{7}Li each split into two hyperfine substates, as shown in figure 2. The ground state hyperfine intervals are known to extremely high accuracy (better than 3 Hz) from magnetic resonance measurements [9]. Selection rules limit two-photon transitions from an S state to $\Delta F = 0$, therefore four atomic transitions are allowed. The two ^{7}Li lines are stronger than the ^{6}Li lines because ^{6}Li accounts for only 7% of natural Li. A sample spectrum is shown in figure 3.

To determine the foreign gas shifts, we measure all four transitions at various buffer gas pressures with the Fabry–Perot wavemeter. The gas pressure is measured with an accuracy of 1% by using a capacitance manometer mounted on the vacuum manifold. The wavenumber of each line is determined from the average of 16 independent measurements. For each measurement we manually set the laser to the peak of the transition. Between measurements the laser is tuned well off the feature and reset to the peak. To minimize bias in setting the laser, we approach the peak alternately from the high energy and low energy sides. Because the wavemeter measures the laser wavenumber, the measurements are multiplied by a factor of two to convert them to the transition energies.

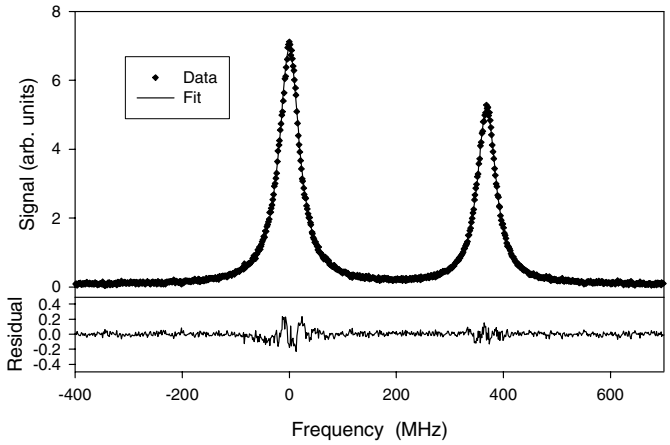

Figure 4. Sample of Lorentzian fit to the ^{7}Li spectra. The frequency scale is the detuning of the laser from the ^{7}Li 2–2 transition. The lower plot shows the residuals.

To measure the line broadening, we scan the laser across the hyperfine transition pair for a single isotope, after determining the transition energies. We assume that the laser scan is linear and obtain a calibration from the measured wavenumbers of the two hyperfine components. This method works satisfactorily because the actual laser scan departs from linearity by less than 2%. Once the scan is calibrated, we fit a pair of Lorentzian profiles to the observed lines, using a generalized least squares technique. This produces well defined values for the line positions and widths. A typical scan and fit are shown in figure 4.

As we reduce the buffer gas pressure, it is necessary to increase the oven heating power to maintain a constant temperature on the wall at the centre of the heat pipe. Maintaining a constant temperature ensures that self-broadening contributions are held constant by keeping the lithium vapour pressure fixed. For all of the data reported here, the wall temperature was maintained at $683.8 \pm 0.3\,^{\circ}$C. The need for increased heating at low buffer gas pressures is probably due to reduced thermal conduction of energy from the hot filament to the pipe wall.

3. Results

Both neon and argon buffer gases shift and broaden the lithium 2S–4S hyperfine transitions. However, the pressure shifts are in opposite directions. This can be seen clearly in figure 5, which shows a series of ^{7}Li spectra recorded at varying pressures for both gases. The amplitudes have been normalized to the same value for ease in comparing widths.

The variation of the transition energies as a function of buffer gas pressure is shown in figures 6 and 7. The error bars represent the standard deviation for each set of data. The trend to larger uncertainties at higher background pressure is due to the increase in the observed linewidths. We did not extend the measurements to still higher pressures because the hyperfine components become unresolved. We obtain the pressure shift rate $\delta\nu$ from a linear least squares fit to the data for each transition and buffer gas. The results are given in table 1. The uncertainties in $\delta\nu$ represent a 68% level of confidence for the fitted value of the slope.

At pressures lower than 40 Pa, the measured transition energy as a function of pressure begins to deviate from linearity. This deviation arises because the system is no longer in a pure foreign gas broadening regime when the buffer gas pressure becomes comparable to the lithium vapour pressure in the centre of the pipe. At $683.8\,^{\circ}$C, the exterior wall temperature

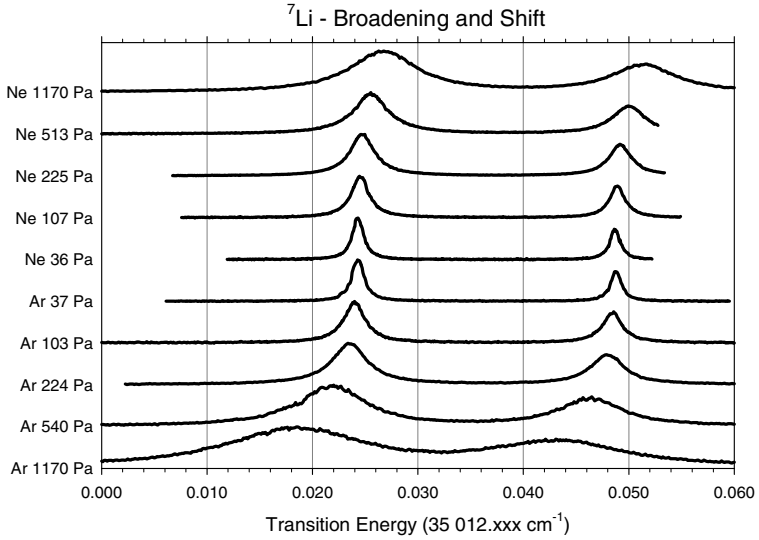

Figure 5. Scans of the ^{7}Li hyperfine pair for Ne and Ar at different pressures. The amplitudes of all of the scans have been normalized to the same arbitrary value.

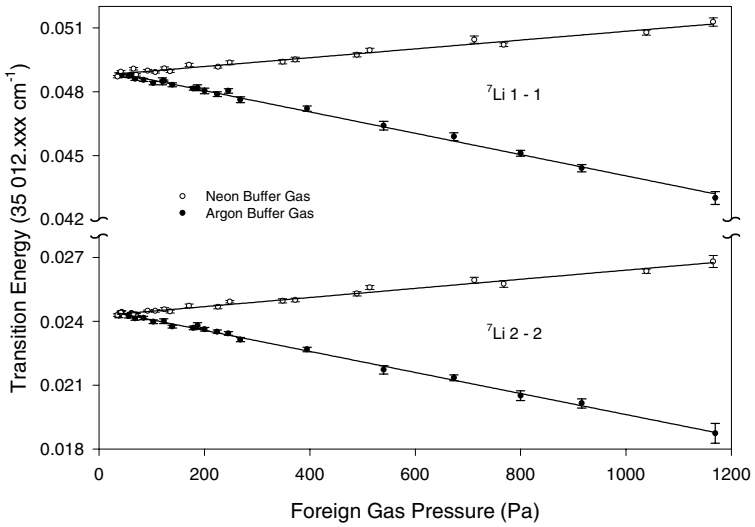

Figure 6. Pressure shift of the ^{7}Li transitions.

of the heat pipe, the lithium vapour pressure would be approximately 40 Pa. We estimate the actual temperature on the inner wall of the pipe to be as much as 15 °C cooler, corresponding to a lithium pressure of about 20 Pa. Spatial variations in the lithium pressure arising from the temperature gradient along the pipe wall further complicate the problem of determining the composition of the vapour in the interaction region. As a result of these effects, it is not possible to extrapolate to zero buffer gas pressure to obtain a determination of the unperturbed transition energies.

The variation of linewidth as a function of pressure is shown for all of the hyperfine transitions in figure 8. There are four contributions to the observed linewidth: natural width, instrumental width (residual Doppler broadening, transit time broadening and laser jitter),

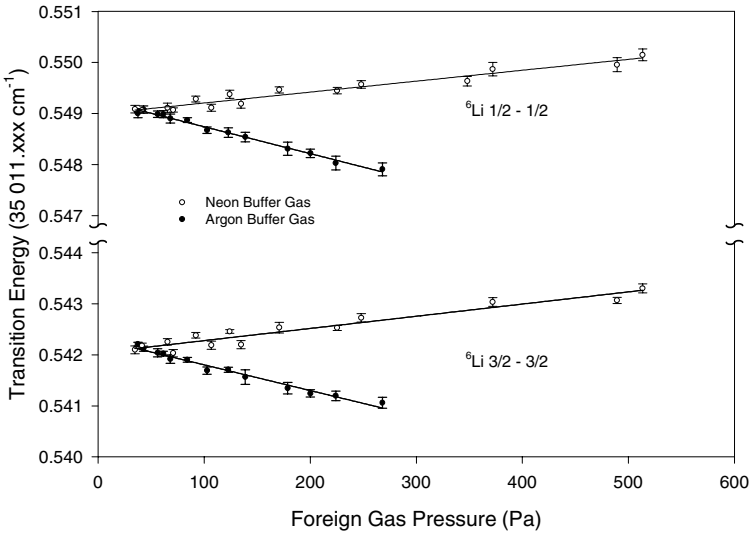

Figure 7. Pressure shift of the ^{6}Li transitions. At higher foreign gas pressures, the hyperfine structure is unresolved.

Table 1. Foreign gas pressure shifts and broadening of the Li 2S–4S hyperfine transitions ($T = 684\,^\circ$C).

Transition	Buffer gas	Pressure shift rate ($\delta\nu$) (MHz Pa^{-1})	Pressure broadening rate ($\delta\gamma$) (MHz Pa^{-1})
^{7}Li $1 \rightarrow 1$	Neon	0.062(2)	0.145(4)
	Argon	−0.148(2)	0.341(3)
^{7}Li $2 \rightarrow 2$	Neon	0.064(2)	0.156(4)
	Argon	−0.150(2)	0.366(4)
^{6}Li $\frac{1}{2} \rightarrow \frac{1}{2}$	Neon	0.064(4)	0.131(3)
	Argon	−0.158(5)	0.305(6)
^{6}Li $\frac{3}{2} \rightarrow \frac{3}{2}$	Neon	0.072(6)	0.135(4)
	Argon	−0.151(7)	0.331(4)

self-broadening and foreign gas broadening. For a fixed heat-pipe temperature, all of these contributions are constant except foreign gas broadening, which is observed to depend linearly on the foreign gas pressure. The largest source of uncertainty in determining the linewidths is the 2% uncertainty in the linearity of the laser scan. The uncertainty arising from calibrating the scan with the measured wavenumbers is at least an order of magnitude smaller, and the uncertainty in the widths arising from the least squares fit to the recorded profiles is negligible. Pressure broadening rates $\delta\gamma$ have been determined for each transition by making a linear least squares fit to the measured linewidths. The results are given in table 1. The uncertainties in $\delta\gamma$ represent a 68% level of confidence for the fitted value of the slope.

At our lowest foreign gas pressure (35 Pa), the observed linewidths are approximately 35 MHz, significantly larger than the natural linewidth of 2.8 MHz. Most of the excess width can be attributed to three sources: residual Doppler broadening, transit time broadening and self-broadening. The combined contribution of transit time broadening and residual Doppler broadening was determined to be 19 ± 2 MHz by removing the focusing lenses and observing the ^{7}Li lines with a collimated beam approximately 2.5 mm in diameter. This is

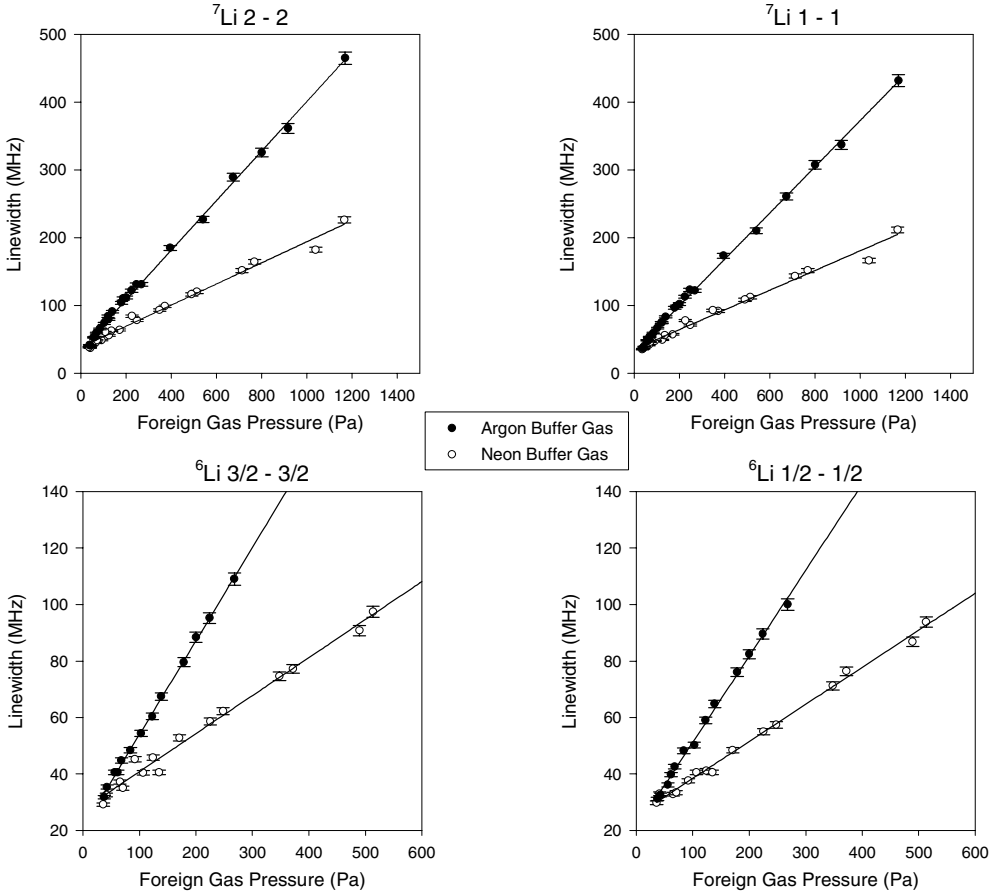

Figure 8. Broadening of the four Li 2S–4S hyperfine transitions.

entirely accounted for by the transit time contribution, which we calculate to be approximately 18.6 MHz. This test also confirms that there is no power broadening contribution to the linewidth, as the laser intensity in the collimated beam is reduced by a factor of nearly 300 from that in the focused beam. The self-broadening contribution was estimated to be 16 ± 3 MHz by measuring the ^{7}Li linewidths as the cell temperature was reduced with 35 Pa of Ne buffer gas. These additional sources of broadening are held fixed during the experiment by maintaining the heat pipe wall at a constant temperature and not changing the optical layout.

4. Discussion

Theoretical treatments of broadening and shift at the low perturber densities used in our experiments are based on the impact approximation [11–16]. In this approximation, the foreign gas broadening and shift are represented by effective cross sections σ' and σ'', which can be calculated assuming an appropriate form for the atom–perturber interaction potential. The linewidth γ and frequency shift ν are given by

$$\gamma = 2N\langle\sigma'_v\rangle\bar{v} \tag{1}$$

and

$$\nu = N\langle\sigma''_v\rangle\bar{v}. \tag{2}$$

Table 2. Comparison of the measured values of the broadening rate $\delta\gamma$ (MHz Pa^{-1}) for both Li hyperfine transitions to the van der Waals model of Wu and Stwalley [14] (at $T = 563$ K) and our calculations based on Kaulakys's semi-classical impact model (Fermi model) [15] and Hermann's modified semi-classical impact model (modified Fermi model) [16] for our experimental conditions.

	^{7}Li			^{6}Li		
		Ne	Ar		Ne	Ar
Experimental	$1 \rightarrow 1$	0.145(4)	0.341(3)	$\frac{1}{2} \rightarrow \frac{1}{2}$	0.131(3)	0.305(6)
	$2 \rightarrow 2$	0.156(4)	0.366(4)	$\frac{3}{2} \rightarrow \frac{3}{2}$	0.135(4)	0.331(4)
van der Waals model [14]		0.62	0.88		—	—
Fermi model [15]		0.124	0.263		0.126	0.281
Modified Fermi model [16]		—	0.295		—	0.316

Table 3. Comparison of the measured values of the shift rate $\delta\nu$ (MHz Pa^{-1}) for both Li hyperfine transitions to the van der Waals model of Wu and Stwalley [14] (at T = 563 K) and our calculations based on Kaulakys's semi-classical impact model (Fermi model) [15] and Hermann's modified semi-classical impact model [16] for our experimental conditions.

	^{7}Li			^{6}Li		
		Ne	Ar		Ne	Ar
Experimental	$1 \rightarrow 1$	0.062(3)	−0.148(2)	$\frac{1}{2} \rightarrow \frac{1}{2}$	0.064(4)	−0.158(5)
	$2 \rightarrow 2$	0.064(2)	−0.150(2)	$\frac{3}{2} \rightarrow \frac{3}{2}$	0.072(6)	−0.151(7)
van der Waals model [14]		−0.15	−0.24		—	—
Fermi model [15]		0.051	0		0.052	0
Modified Fermi model [16]		—	−0.160		—	−0.171

Here N is the foreign gas number density and $\bar{v}$ is the average relative velocity of the interacting atoms given by

$$\bar{v} = \sqrt{\frac{8kT}{\pi\mu}} \tag{3}$$

where μ is the reduced mass. The thermally averaged cross sections $\langle\sigma_v'\rangle$ and $\langle\sigma_v''\rangle$ are determined by integrating the effective cross sections over the Maxwell velocity distribution:

$$\langle\sigma_v\rangle = \frac{\langle v\sigma(v)\rangle}{\langle v\rangle}. \tag{4}$$

We compare our experimental broadening and shift rates with theoretical values determined by using three different models for the calculation of the effective cross sections.

Wu and Stwalley [14] modelled the perturbation of two-photon transitions in alkali metals by rare gases using van der Waals interaction potentials. Their calculations of the broadening and shift rates, $\delta\gamma$ and $\delta\nu$, for the 2S–4S transition in Li at a temperature of 563 K are shown in tables 2 and 3. The values of $\delta\gamma$ predicted by this model are larger than the experimental results by factors of 2.5–4. The calculated value of $\delta\nu$ is significantly overestimated for the Li–Ar system and has the wrong sign for Li–Ne. For the case of Na–Ne, Wu and Stwalley [14] attributed the incorrect sign they obtained to short range repulsive forces that are not included in the model. These repulsive forces are very significant for light rare gases, which have small polarizabilities.

Kaulakys [15] used a superposition of attractive polarization potentials with a repulsive Fermi contact pseudopotential to derive improved expressions for broadening and shift cross

Table 4. Dipole polarizability α [24], scattering length L [25] and slope range r_s [16] used in the semi-classical impact models. The critical quantum numbers n_1^* and n_2^* are calculated from equation (25) of [15].

	Ne	Ar
α (a_0^3)	2.663	11.08
L (a_0)	0.204	−1.55
r_s (a_0)	—	12
n_1^*	2.86	4.66
n_2^*	4.13	7.31

sections. His results agree well with experiment for the interaction of Na and Cs with all of the rare gases except Ne, over a wide range of principal quantum numbers. We used the Kaulakys model to calculate broadening and shift rates for Li perturbed by Ne and Ar under our experimental conditions. The thermally averaged broadening cross sections $\langle\sigma_v'\rangle$ are given by equations (35) and (36) of [15]. Thermally averaged shift cross sections $\langle\sigma_v''\rangle$ for the Kaulakys model are given by equations (3a) and (3b) of [22]. From these formulae and equations (1)–(3) above we calculate values of $\delta\gamma$ and $\delta\nu$ using the parameters summarized in table 4. The results are shown in tables 2 and 3.

The values of $\delta\gamma$ calculated with the Kaulakys model are in much better agreement with experiment than those calculated using the van der Waals model but still differ from the experimental results by as much as 40%. Also, for both Ne and Ar the predicted isotopic dependence of $\delta\gamma$ does not agree well with experiment. The broadening rates, which are predicted to be greater for ^{6}Li, are actually observed to be greater for ^{7}Li. For $\delta\nu$, the predicted values are within 30% of the experimentally measured shift rates for the Li–Ne system. For the case of Li–Ar, however, the model incorrectly predicts no shift of the lithium transitions as a function of argon pressure.

Hermann [16, 23] has noted that when the effective quantum number n^* is less than the first critical quantum number n_1^* (as is the case for Li–Ar), the combination of Fermi pseudopotential and JWKB wavefunction used by Kaulakys introduces a discontinuity in the collisional phase shift. This results in an underestimation of the broadening cross section. To handle this case, Hermann introduced a modified Fermi potential, that produces a linear smoothing of the discontinuity. Expressions for the resulting broadening and shift cross sections for $n^* < n_1^*$ are given in equations (24) and (25) of [16]. Thermally averaging these cross sections (again using the parameters in table 4), we calculate for Li–Ar the broadening and shift rates shown in tables 2 and 3. The modified Fermi potential is quite successful, producing shift rates that are within 10% of the experimental values. The results for the Li–Ar broadening rates are also clearly improved, with agreement for most of the lines at better than 20%.

We are not aware of any previous experimental studies of foreign gas broadening and shifts for two-photon transitions in lithium, although there have been several studies of these transitions in Na [17–19], Rb [20–22] and Tl [23].

In the previous studies of alkali two-photon transitions, broadening and shift rates have not been reported for individual hyperfine components. For the Na 3S–4D and 3S–5S transitions, Biraben *et al* [17] state that the shift and broadening rates were verified to be the same for all hyperfine components. Brillet and Gallagher [20] also found that the broadening and shift rates were independent of the hyperfine component in their study of two-photon transitions in Rb.

Omont [26] has predicted that broadening and shift rates for a transition can depend upon the rank of the transition operator if the total angular momenta J of both the initial and final

states are greater than or equal to one and if both states are significantly perturbed by the interaction. Under these same conditions, hyperfine components of a transition may display differing rates. These predictions were tested explicitly for the $6\,^2P_{3/2}$–$9\,^2P_{3/2}$ transition of Tl by Hermann *et al* [23]. No dependence of the broadening and shift rates on either the rank of the transition operator or on hyperfine component was observed.

In our experiment, the shift rates for Li perturbed by Ne and Ar and the broadening rates for Ne show no dependence on hyperfine component. In contrast to previous experiments, however, our broadening rates for Li perturbed by Ar (table 1) do depend significantly on hyperfine component. For both Li isotopes, the Ar broadening rates differ for the two hyperfine components by four to five times the combined uncertainties. This is an unexpected result, as neither of the conditions stated by Omont are realized for the Li 2S–4S transition.

5. Conclusions

We have measured the foreign gas shift and broadening for all hyperfine components of the Li 2S–4S two-photon transition in a heat-pipe oven with Ne and Ar buffer gases. As expected, the linewidth and shift depend linearly on the buffer gas pressure. Broadening and shift rates are determined with an accuracy of 5% or better for most of the components.

Calculations in the impact approximation using a superposition of polarization and modified Fermi potentials to model the lithium–rare gas interaction [15, 16] are in quantitative agreement with the experimental results at a level of 10–30%. The calculations, however, fail to reproduce two qualitative features of the data. First, the broadening rates measured for ^{7}Li are approximately 10% greater than for ^{6}Li instead of slightly smaller as predicted by the model. Second, the broadening rates measured for perturbation of Li by Ar are different for the two hyperfine components of each isotope.

Acknowledgment

The authors would like to acknowledge Damir Veza for providing guidance on using thermionic diodes as well as fruitful discussions on the theory of foreign gas broadening and shifts.

References

[1] King F W 1997 *J. Mol. Struct. (Theochem)* **400** 7
[2] King F W 1999 *Adv. At. Mol. Opt. Phys.* **40** 57
[3] Niemax K 1985 *Appl. Phys.* B **38** 147
[4] Sansonetti C J 1988 *Advances in Laser Science* vol 4, ed J L Gole *et al* (New York: American Institute of Physics) p 548
[5] Gillaspy J D and Sansonetti C J 1991 *J. Opt. Soc. Am.* B **8** 2414
[6] Sansonetti C J 1997 *J. Opt. Soc. Am.* B **14** 1913
[7] Layer H P 1980 *IEEE Trans. Instrum. Meas.* **29** 358
[8] Jennings D A, Pollock C R, Petersen F R, Drullinger R E, Evenson K M, Wells J S, Hall J L and Layer H P 1983 *Opt. Lett.* **8** 136
[9] Beckmann A, Böklen K D and Elke D 1974 *Z. Phys.* **270** 173
[10] DeGraffenreid W and Sansonetti C J 2003 *Phys. Rev.* A **67** 012509
[11] Fermi E 1934 *Nuovo Cimento* **11** 157
[12] Alekseev V A and Sobel'man I I 1966 *Sov. Phys.–JETP* **22** 882
[13] Omont A 1977 *J. Physique* **38** 1343
[14] Wu C Y R and Stwalley W C 1978 *Phys. Rev.* A **18** 1066
Wu C Y R and Stwalley W C 1981 *Phys. Rev.* A **24** 1117
[15] Kaulakys B 1984 *J. Phys. B: At. Mol. Phys.* **17** 4485

[16] Hermann G 1988 *Phys. Lett.* A **133** 225
[17] Biraben F, Cagnac B, Giacobino E and Grynberg G 1977 *J. Phys. B: At. Mol. Phys.* **10** 2369
[18] Flusberg A, Kachru R, Mossberg T and Hartmann S R 1979 *Phys. Rev.* A **19** 1607
[19] Kachru R, Mossberg T W and Hartmann S R 1980 *Phys. Rev.* A **21** 1124
[20] Brillet W-Ü L and Gallagher A 1980 *Phys. Rev.* A **22** 1012
[21] Weber K H and Niemax K 1982 *Z. Phys.* A **307** 13
[22] Thompson D C, Kammermayer E, Stoicheff B P and Weinberger E 1987 *Phys. Rev.* A **36** 2134
[23] Hermann G, Kaulakys B and Mahr G 1998 *Eur. Phys. J.* D **1** 129
[24] Teachout R R and Pack R T 1971 *At. Data* **3** 195
[25] Golovanivskiĭ K S and Kabilan A P 1981 *Sov. Phys.–JETP* **53** 1153
[26] Omont A 1973 *J. Physique* **34** 179